Redox Biology 28 (2020) 101329

Contents lists available at ScienceDirect

Redox Biology

journal homepage: www.elsevier.com/locate/redox

Short Communication

Gestational oxidative stress protects against adult obesity and insulin resistance

Lidiya G. Dimova[a], Simone Battista[a], Torsten Plösch[b], Rosalie A. Kampen[a], Fan Liu[a,d], Rikst Nynke Verkaik-Schakel[b], Domenico Pratico[c], Henkjan J. Verkade[a], Uwe J.F. Tietge[a,d,e,*]

[a] Department of Pediatrics, University of Groningen, University Medical Center Groningen, Hanzeplein 1, Groningen, the Netherlands
[b] Department of Obstetrics and Gynecology, University of Groningen, University Medical Center Groningen, Hanzeplein 1, Groningen, the Netherlands
[c] Alzheimer's Center at Temple, Lewis Katz School of Medicine, Temple University, 3500 N Broad St, Philadelphia, PA, USA
[d] Division of Clinical Chemistry, Department of Laboratory Medicine, Karolinska Institutet, Alfred Nobels Alle 8, Stockholm, Sweden
[e] Clinical Chemistry, Karolinska University Laboratory, Karolinska University Hospital, Stockholm, Sweden

ARTICLE INFO

Keywords:
Fetal oxidative stress
Mitohormesis
Metabolic programming
Adiposity
Epigenetics
Methylation

ABSTRACT

Pregnancy complications such as preeclampsia cause increased fetal oxidative stress and fetal growth restriction, and associate with a higher incidence of adult metabolic syndrome. However, the pathophysiological contribution of oxidative stress *per se* is experimentally difficult to discern and has not been investigated. This study determined, if increased intrauterine oxidative stress (IUOx) affects adiposity, glucose and cholesterol metabolism in adult Ldlr−/−xSod2+/+ offspring from crossing male Ldlr−/−xSod2+/+ mice with Ldlr−/−xSod2 +/- dams (IUOx) or Ldlr−/−xSod2 +/- males with Ldlr−/−xSod2+/+ dams (control). At 12 weeks of age mice received Western diet for an additional 12 weeks. Adult male IUOx offspring displayed lower body weight and reduced adiposity associated with improved glucose tolerance compared to controls. Reduced weight gain in IUOx was conceivably due to increased energy dissipation in white adipose tissue conveyed by higher expression of Ucp1 and an accompanying decrease in DNA methylation in the Ucp1 enhancer region. Female offspring did not show comparable phenotypes. These results demonstrate that fetal oxidative stress protects against the obesogenic effects of Western diet in adulthood by programming energy dissipation in white adipose tissue at the level of Ucp1.

1. Introduction

Epidemiological evidence indicates that stressful environmental conditions during sensitive periods of early development predispose to chronic disease later in life [1]. Preeclampsia and intrauterine growth restriction (IUGR) are particular manifestations of fetal stress associated with a higher incidence of visceral obesity [2], hypertension and heart disease [1] in adulthood. A common denominator of these adverse perinatal conditions is intrauterine oxidative stress (IUOx) [3]. Oxidative stress could thereby be a mere accompanying feature or the driving force for metabolic programming. Increased levels of reactive oxygen species (ROS) mechanistically contribute to atherosclerotic plaque formation [4] and pancreatic β-cell dysfunction [5]. However, the involvement of oxidative stress in fetal programming of the metabolic syndrome has not been investigated. Since IUOx often co-manifests with IUGR, defining the role of oxidative stress *per se* is challenging. To address the specific impact of segregated IUOx on metabolic syndrome components in adulthood we devised a genetic mouse model where IUOx is not associated with either IUGR, maternal obesity or diabetes. Specifically, we used Mn^{2+}-superoxide dismutase (Sod2) deficient mice, in which oxidative stress is significantly increased even in a heterozygous state [6]. Our results demonstrate that, independent of fetal weight, increased IUOx *in utero* epigenetically programs protection against diet-induced adiposity, insulin resistance and hyperlipidemia in Sod2-wild-type male offspring of Sod2-deficient mothers. Conceivably, this protection is mediated by increased energy expenditure due to browning of WAT as indicated by higher Ucp1 expression concomitant with reduced methylation of its enhancer.

* Corresponding author. Division of Clinical Chemistry, Department of Laboratory Medicine (LABMED), H5, Alfred Nobels Alle 8, Karolinska Institutet, S-141 83, Stockholm, Sweden.
E-mail addresses: u_tietge@yahoo.com, uwe.tietge@ki.se (U.J.F. Tietge).

https://doi.org/10.1016/j.redox.2019.101329
Received 14 December 2018; Received in revised form 11 September 2019; Accepted 15 September 2019
Available online 17 September 2019

2. Materials and methods

2.1. Animal experiments

Mice heterozygous for Sod2^{tm1Leb} and homozygous for Ldlr^{tm1Her} (#006883, Jackson Laboratories, Bar Harbor, USA) were crossed with Ldlr-knockouts (#002207). Thus, all studied mice are homozygous Ldlr-knockouts (−/−). IUOx are Sod2 (+/+) offspring originating from mating Sod2 (+/-) females with Sod2 (+/+) males. Controls originated from Sod2 (+/+) females mated with Sod2 (+/-) males. Animals were co-housed in temperature-controlled conditions with 12:12 h light/dark cycles with ad libitum access to AIN93G semisynthetic diet (#D10012G, Research Diets, USA). At 12 weeks of age experimental animals received Western diet containing 60% fat and 0.25% cholesterol (#D14010701, Research Diets). Complete diet composition is provided in Supplementary Table 2. Supplementary Fig. 3 summarizes the timeline of the study.

2.2. Body composition analysis

Body composition measurements were performed by dual energy x-ray absorptiometry (pDEXA, Norland-Stratec, Norland Medical Systems Inc., UK). During the procedure the animals were anesthetized with isoflurane for a total of 15 min. Fat and lean body mass were calculated based on the automated bone mass density evaluation.

2.3. Fat balance

The fat absorption efficiency was determined as the difference between dietary intake of long chain fatty acids and their amount recovered from feces. Fatty acids were methylated and extracted from food and fecal samples as previously described [7] followed by gas chromatography analysis. The free fatty acid concentrations of the species 14:0 to 26:0 per gram of sample were calculated relative to a 17:0-internal standard.

2.4. Glucose tolerance test and insulin measurement

Following a 12 h overnight fast mice were injected i.p. with 1.25 g/kg D-glucose and blood glucose was measured before and 15, 30, 60 and 120 min after the injection using OneTouch Ultra glucose strips (12%CV, Life Scan, USA). Fifteen minutes after the glucose injection plasma samples were collected for determination of circulating insulin levels (Ultrasensitive Insulin ELISA Kit, Crystal Chem, USA). HOMA-IR was calculated as described [8].

2.5. Plasma lipids and lipoprotein profiles

Blood was collected via retro-orbital bleeding under isoflurane anesthesia. Samples were centrifuged at 500 × *g*, 4C° for 10 min. Total cholesterol and triglycerides were measured with colorimetric kits (13%CV #11489232 and 14.5%CV #11877771, Roche, Germany). Pooled plasma samples (n = 4–5/group) were loaded onto a Superose 6 H R 10/300 GL column (GE Healthcare, UK) for lipoprotein separation via fast protein liquid chromatography (FPLC) as described [9].

2.6. Fecal neutral sterols and bile acids

Feces were dried, weight and ground. Neutral sterol and bile salt profiles were determined exactly as previously described [10]. Following petroleum ether extraction neutral sterols were measured in the organic phase by gas chromatography. Total bile acids were determined by gas chromatography in the aqueous phase after concentration with SepPak® C18 cartridges (Waters, USA).

2.7. Isoprostane determination

Samples underwent extraction by use of a C18 cartridge and then were purified by thin-layer chromatography. Next, 8-isoPGF2alpha levels were assayed by a specific and sensitive sandwich ELISA method, as previously described [11].

2.8. RT-qPCR

RNA was isolated from frozen tissues using Trizol® (Thermo Fischer Scientific, USA) and quantified with a NanoDrop 2000 (Thermo Fischer Scientific). cDNA synthesis and real-time PCR quantification of gene expression levels were performed as previously detailed [10].

2.9. ELISA

In plasma, levels of SAA (MyBioSource, San Diego, CA, MBS2500351) and of the proinflammatory cyto- and chemokines (all R &D Systems, Minneapolis, MN) Il-6 (M6000B), Tnf-α (MTA00B), Il-1β (MLB00C) and Ccl2 (MJE00B) were determined following the manufacturer's instructions.

2.10. DNA methylation analysis

DNA methylation analysis was performed as described (*24*). Briefly, genomic DNA from WAT (170 ng) was bisulfite-converted with the EZ DNA Methylation-Gold kit (Zymo Research, USA). Bisulfite-specific primers were designed with the PyroMark Assay Design software for CpG positions located in the Ucp1 enhancer and promoter (Supplementary Table 1). The methylation status was analyzed by pyrosequencing (PyroMarkQ24, Qiagen). PyroMarkQ24 software was used to determine the methylation percentage of individual CpG positions.

2.11. Statistical analysis

Statistical analysis was performed using Graph Pad Prism 6.0. Data are presented as median and interquartile range. Differences between groups were calculated using Mann-Whitney or Kruskal-Wallis followed by post-hoc Tukey, or repeated measures ANOVA followed by Fischer's exact test. P-values ≤ 0.05 were considered statistically significant.

2.12. Study approval

All animal experiments comply with the ARRIVE guidelines and were approved by the IACUC at the University of Groningen with permit DEC6493AB.

3. Results

3.1. Maternal Sod2-heterozygosity causes fetal oxidative stress but not IUGR

Full ablation of SOD2 is lethal, and heterozygosity results in IUGR [12]. However, here we focused exclusively on SOD2-wild-type offspring, where fetal weight (E18.5) was not different between pups originating from SOD2$^{+/-}$ dams versus SOD2$^{+/+}$ dams (Fig. 1A & Supplementary Fig. 1A). Hence, in our model adult phenotypes occur independent of IUGR. Levels of the oxidative stress marker isoprostane 8-isoPGF2*α* were significantly higher in IUOx pups (Fig. 1B & Supplementary Fig. 1B) demonstrating that indeed maternal SOD heterozygosity causes increased oxidative stress exposure *in utero* in both sexes. The increase in isoprostanes in female IUOx pups was lower than in males, likely due to a higher oxidative stress buffering capacity of the female placenta, since mRNA expression of SOD1 (1.00 ± 0.08 vs. 0.76 ± 0.05, p < 0.05) and catalase (1.00 ± 0.05 vs. 0.84 ± 0.04,

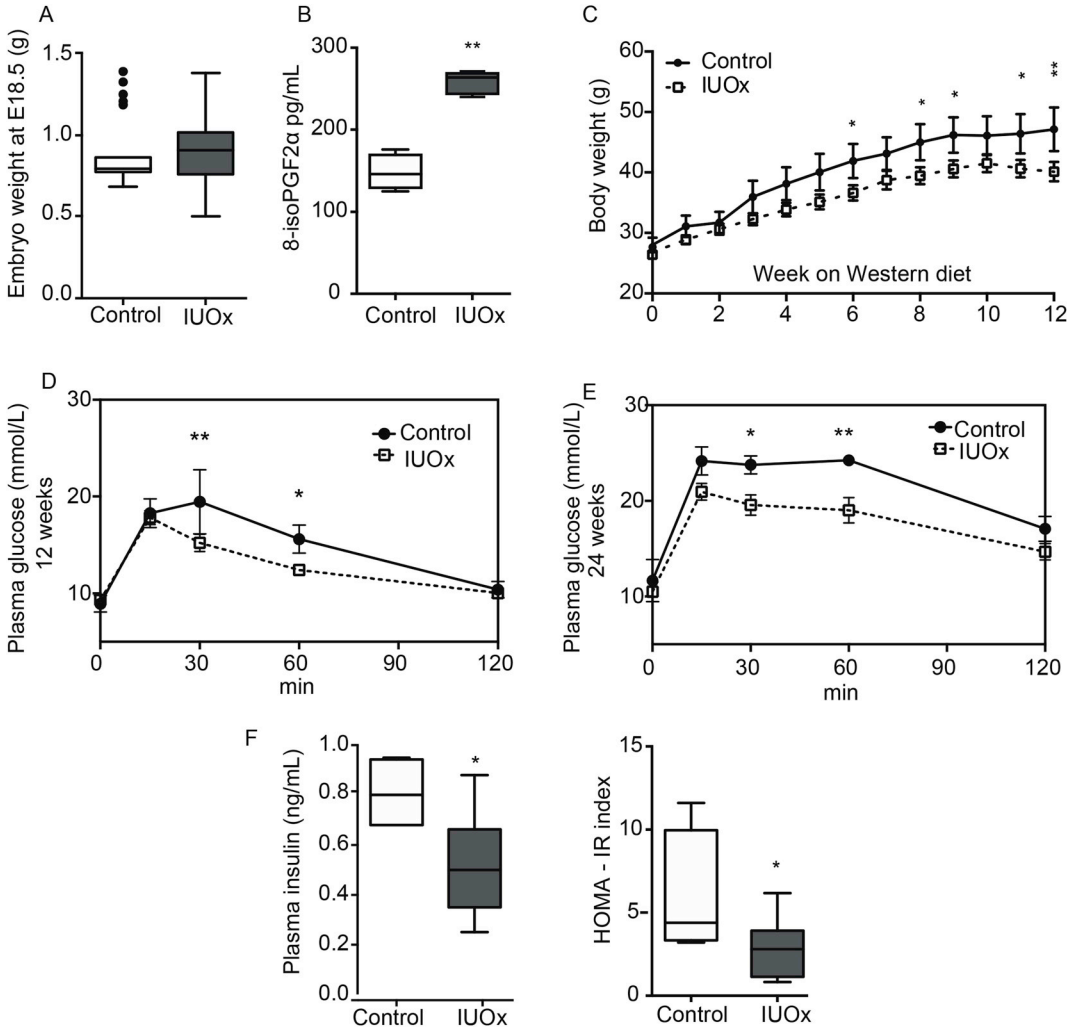

Fig. 1. IUOx protects against diet-induced obesity and insulin resistance in adulthood. A) Embryonic weight of male *Ldlr −/− Sod2 + / +* offspring at 18.5 days. N > 12/group. **B**) Oxidative stress marker 8-isoPGF2α in plasma of male *Ldlr −/− Sod2 + / +* offspring at 18.5 days (n = 6/group). Data are given as median and interquartile range. Mann-Whitney *U* test. **C**) Body weight trajectories from the start of Western diet feeding until 24 weeks of age. **D**) Glucose tolerance test in 12 week old offspring fed chow diet. **E**) Glucose tolerance test at 24 weeks, after 12 weeks on Western diet. Repeated measures ANOVA posthoc Fischer's exact test. **F**) Glucose-induced insulin secretion after 12 weeks of Western diet and HOMA-IR after 12 weeks on WD. Data are given as median and interquartile range; males, n = 4–5/group. Mann-Whitney *U* test. *p < 0.05, **p < 0.01.

p < 0.05) was higher in female compared with male IUOx placentas.

3.2. IUOx exposure results in reduced body weight gain and glucose tolerance in adult male offspring

At 12 weeks of age SOD2-wild-type offspring were subjected to a Western diet challenge. Although body weight of IUOx and controls were identical at the start of the diet, from week 6 onwards IUOx mice gained significantly less weight during the whole experiment (Fig. 1C). Notably, this effect was observed only in male offspring while females had comparable weight gain (Supplementary Fig. 1C). Lower body weight associates with better glucose tolerance [13]. However, already before starting the Western diet, at 12 weeks of age when body weights did not differ, IUOx-males showed a trend towards improved glucose tolerance (Fig. 1D) compared to controls in intraperitoneal glucose tolerance tests. After 12 weeks on Western diet both groups had become more glucose intolerant (Fig. 1E) than prior to the challenge. However, IUOx-males were still more glucose tolerant than controls (Fig. 1D–E). Circulating insulin was also lower (p < 0.05) in IUOx-mice (Fig. 1F, left) resulting in a decreased HOMA-IR (p < 0.05, Fig. 1F, right). Females did not show such differences in glucose tolerance (Supplementary Fig. 1D).

When IUOx males were continued on a chow diet until 24 weeks of age, blood glucose, insulin and HOMA-IR were not different compared to controls (data not shown). Hepatic expression of the acute phase protein SAA was also comparable between groups as were plasma levels of SAA and Ccl2; Il-6, Il-1β and Tnf-α were not detectable in plasma of either IUOx or control offspring (data not shown).

3.3. IUOx results in lower plasma cholesterol in adult male offspring

LDLR-knockout mice develop diet-induced hyperlipidemia [14]. At 24 weeks of age, IUOx males had 22% lower fasting total plasma cholesterol compared to controls (p < 0.05, Fig. 2A), and lower plasma TG (p = 0.075, Fig. 2B). This reduction was mostly due to lower cholesterol within Apo-B containing lipoproteins (Fig. 2C). Next, we investigated fecal sterol excretion. While cholesterol recovered from feces was comparable between groups (Fig. 2D), fecal bile acid output was higher in IUOx mice (Fig. 2E) suggesting an overall improved cholesterol excretion. Such effects on plasma lipids and fecal sterol excretion were absent in female offspring (Supplementary Figs. 1E–F).

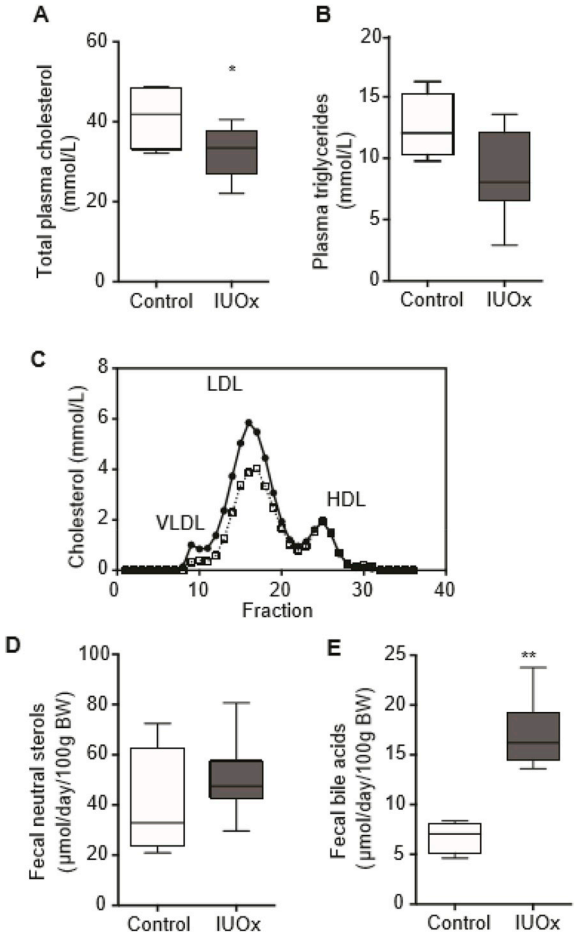

Fig. 2. IUOx protects against the effects of Western diet on cholesterol metabolism. A) Total plasma cholesterol levels and **B**) plasma triglycerides at 24 weeks of age. Data are given as median and interquartile range; n = 4–5/group, Mann-Whitney *U* test. **C**) Cholesterol distribution over the different lipoprotein fractions following FPLC separation of pooled plasma samples of at least 4 mice/group at the age of 24 weeks. **D**) Fecal neutral sterol and **E**) total fecal bile acid excretion at 24 weeks of age. Data are presented as median and interquartile range, n = 4–5/group, Mann-Whitney *U* test, *p < 0.05., **p < 0.01.

3.4. Male IUOx offspring display reduced adiposity due to browning of white adipose tissue

Body composition analysis at 24 weeks revealed a markedly reduced adipose tissue mass in IUOx males (Fig. 3A); lean body mass was not different (data not shown). Decreased adiposity could be explained by either lower caloric intake, decreased absorption or increased energy expenditure. Caloric intake (Fig. 3B) and fat absorption (Fig. 3C) were comparable. As surrogate parameters for energy expenditure, we measured mRNA expression levels of genes associated with increased energy dissipation in brown (BAT) and white adipose tissue (WAT). Ucp1 is a key mediator of increased energy expenditure [15]. Usually expressed in BAT in a Pparg co-activator 1a (Pgc1a)-dependent manner, its upregulation in WAT, the so-called 'browning', decreases obesity [16]. We observed a marked 3-fold induction of Ucp1 mRNA (p = 0.05) in WAT of IUOx males (Fig. 3D), while Ucp1 expression in BAT did not change. This observation lends strong support to a causative contribution of the higher Ucp1 expression in WAT of male IUOx mice to the improved metabolic state in this group. In female offspring expression levels of Ucp1 were comparable between controls and IUOx consistent with the lack of differential weight gain (Supplementary Fig. 1G). The lack of differential expression of Ucp1 in female offspring, where a long-term metabolic impact of intrauterine oxidative stress was missing, supports a critical role for Ucp1 in conveying the protective effects of IUOx.

3.5. Pgc1a-independent mechanisms determine increased Ucp1 expression in adulthood following intrauterine oxidative stress exposure

Ucp1 upregulation in WAT was previously described in Pparg knockout mice resistant to diet-induced obesity [17]. However, expression of both Pparg and its model target gene Cd36, responsible for fatty acid uptake, were comparable between IUOx and control mice in different tissues (Supplementary Fig. 2A), indicating that likely Pparg is not causally involved in Ucp1 regulation in our model. The expression levels of Ucp1 can also be modulated by reactive oxygen species [18]. We hence measured the expression of key genes involved in regulating oxidative metabolism, such as Pgc1a, which mediates Ucp1-dependent adaptive thermogenesis in BAT [19]. However, Pgc1a expression was identical between IUOx and control males (Supplementary Fig. 2B) suggesting another, likely epigenetic, mechanism to underlie the regulation of Ucp1 expression in response to IUOx.

3.6. Differential methylation at the Ucp1 enhancer region associates with altered UCP-1 expression in white adipose tissue

Earlier work identified several CpG positions in the Ucp1 gene enhancer and promoter region [20]. To test whether these (Fig. 3E) are sensitive to IUOx, we analyzed them in WAT of IUOx and controls. While the Ucp1 promoter was not differentially methylated (Supplementary Fig. 2C), CpG2 in the enhancer region was significantly less methylated specifically in male IUOx mice (Fig. 3F). Similar effects in Ucp1 expression or gene methylation were absent in female IUOx compared with control offspring (Supplementary Fig. 1H).

Combined these data suggest that IUOx exposure results in differential methylation at the Ucp1 locus in a sexually dimorphic fashion. These epigenetic changes confer protection against the adverse metabolic effects of Western diet in male offspring via browning of WAT.

4. Discussion

Although clinically and epidemiologically relevant, it is difficult in a human system to determine effects of intrauterine oxidative stress exposure on the offspring, since oxidative stress is almost inevitably mixed with other conditions such as IUGR that by themselves impact programming of metabolic disease [1]. In contrast, the mouse model described in this study allowed us to investigate the specific impact of IUOx on metabolic phenotypes in adult life. Combined, our data suggest that IUOx exposure results in differential methylation at the Ucp1 locus in a sexually dimorphic fashion. These epigenetic changes confer protection against the adverse metabolic effects of Western diet in male offspring via browning of WAT.

How can a supposedly adverse factor such as increased ROS confer protection against diet-induced metabolic dysfunction? In general, obesogenic diets and increased adiposity are associated with higher levels of systemic oxidative stress. Moderate levels of ROS, however, also fulfill an important physiological role in regulating gene expression and cell signaling pathways governing e.g. fetal development and vascularization [21]. Also, relevant beneficial effects of exercise are largely conveyed by increased oxidative stress which mitigates insulin resistance by altering the expression of ROS-sensitive transcriptional regulators of glucose homeostasis such as Pparg and Pgc1a [22]. From these and similar observations the concept of "mitohormesis" developed [23]. It suggests that exposure to small doses of a stressor such as ROS, can protect against larger subsequent doses. In our model, increased intrauterine ROS exposure appears to condition metabolic networks towards an improved response to an increasing oxidative and nutritional burden associated with the Western diet in adulthood. While

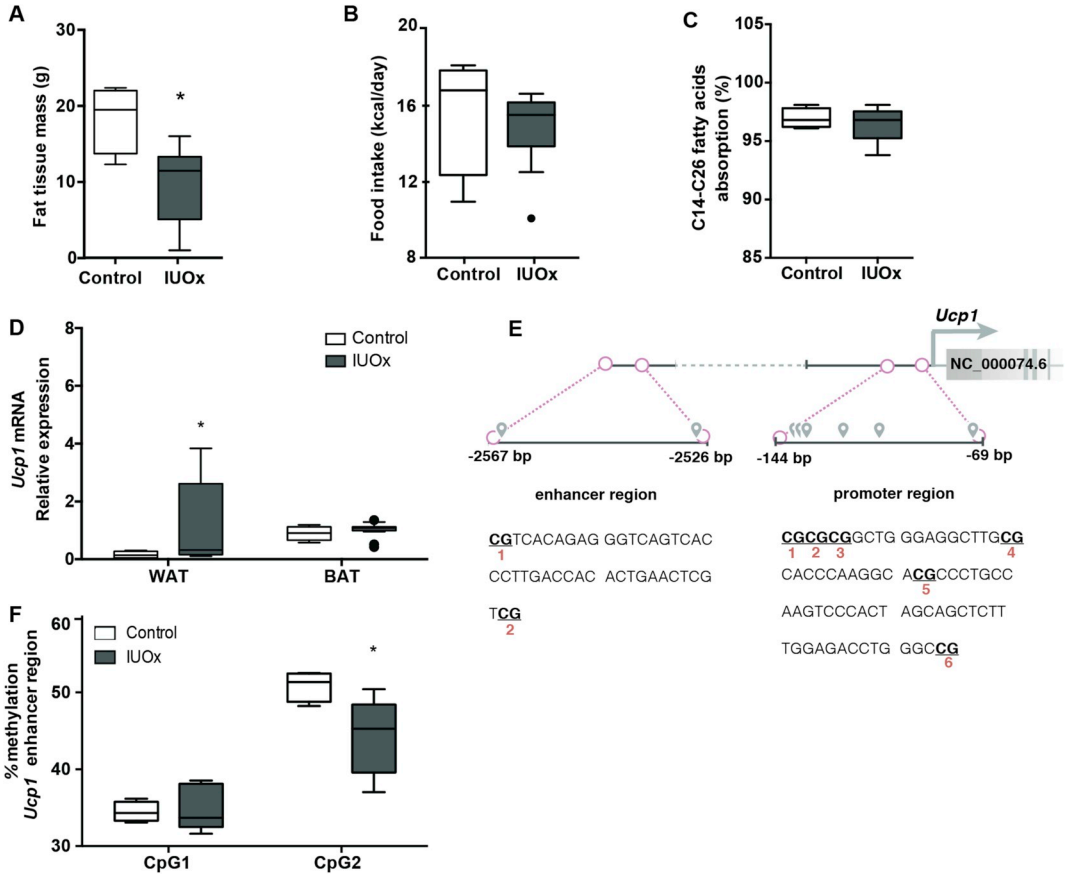

Fig. 3. IUOx reduces body fat content by increasing energy dissipation via epigenetic upregulation of Ucp1 in WAT. **A**) Body fat quantification via pDEXA at 24 weeks of age, after 12 weeks of Western diet feeding. **B**) Food intake based on averaged values over 3 consecutive days. **C**) Long-chain fatty acid absorption. **D**) Ucp1 mRNA expression levels in white and brown adipose tissue. **E**) Schematic of the CpG dinucleotides localization in the Ucp1 enhancer and promoter regions. **F**) DNA methylation state of individual CpG pairs located in the enhancer region of Ucp1. Data are presented as median and interquartile range, n = 4–5/group, Mann-Whitney *U* test, *p < 0.05.

we are not aware of comparable studies in a mammalian system, work in Drosophila indicated that increased oxidative stress due to hyperbaric pressure in early development resulted in increased resistance to oxidative stress in adult flies and an extended lifespan [24]. Hyperbaric oxygen chambers are in use as treatment for severe IUGR due to placental insufficiency [25]. This improves short-term outcomes, however, long-term metabolic effects have not been systematically addressed.

One relatively frequent finding of metabolic programming studies is the sex-specificity of the offspring's phenotype. Embryonic sex can modulate placental size, function and ability to respond to adverse stimuli [26]; hence sex-specific placental differences are proposed to contribute to the sexual dimorphism in programming. Recently several gender-specific placental differences in response to oxidative stress were shown in the guinea pig [27]. The difference we observed in isoprostane levels between male and female fetuses in the IUOx group potentially relates to the anthropomorphic and physiological changes between the genders in adult age and is, based on the lower expression of catalase and Sod1, likely conveyed by a decreased placental anti-oxidative defense in males.

In summary, our data demonstrate that intrauterine oxidative stress exposure results in resistance to diet-induced adiposity, glucose intolerance and dyslipidemia in adult mice. This response is restricted to male offspring. Mechanistically, this protective effect is conveyed by programming of energy dissipation in WAT via increased expression of Ucp1, at least partly mediated by decreased DNA methylation in its enhancer region. These data might have important implications also for interpreting the effects of oxidative stress during pregnancy on programming of metabolic disease in humans.

Funding sources

This work was supported by the Dutch Technology Foundation STW (www.stw.nl, grant: 11675) and was partly funded by Danone Nutricia Research. STW is now part of the Netherlands Organisation for Scientific Research.

Author contributions

LGD performed animal experiments, data acquisition and analysis, drafting of the manuscript. SB assisted in animal experiments and data acquisition, RAK, LF, DP acquired, analyzed and interpreted data, RNVS and TP performed the methylation analysis. HJV supervised experiments, interpreted data, reviewed/edited the manuscript. UJFT conceived the study, designed and supervised the experiments, interpreted data, reviewed/edited the manuscript.

Conflicts of interest

The authors have declared that no conflict of interest exists.

Appendix A. Supplementary data

Supplementary data to this article can be found online at https://doi.org/10.1016/j.redox.2019.101329.

References

[1] D.J. Barker, The fetal and infant origins of disease, Eur. J. Clin. Investig. 25 (1995) 457–463.
[2] J.L. Morrison, J.A. Duffield, B.S. Muhlhausler, et al., Fetal growth restriction, catch-up growth and the early origins of insulin resistance and visceral obesity, Pediatr. Nephrol. 25 (2010) 669–677.
[3] L.P. Thompson, Y. Al-Hasan, Impact of oxidative stress in fetal programming, J. Pregnancy 2012 (2012) 582748.
[4] D. Harrison, K.K. Griendling, U. Landmesser, et al., Role of oxidative stress in atherosclerosis, Am. J. Cardiol. 91 (2003) 7A–11A.
[5] X. Wang, H. Li, D. De Leo, et al., Gene and protein kinase expression profiling of reactive oxygen species-associated lipotoxicity in the pancreatic beta-cell line MIN6, Diabetes 53 (2004) 129–140.
[6] J.E. Kokoszka, P. Coskun, L.A. Esposito, et al., Increased mitochondrial oxidative stress in the Sod2 (+/-) mouse results in the age-related decline of mitochondrial function culminating in increased apoptosis, Proc. Natl. Acad. Sci. U. S. A. 98 (2001) 2278–2283.
[7] F.A. Muskiet, J.J. van Doormaal, I.A. Martini, et al., Capillary gas chromatographic profiling of total long-chain fatty acids and cholesterol in biological materials, J. Chromatogr. B: Biomed. Sci. Appl. 278 (1983) 231–244.
[8] T.H. van Dijk, A.J. Laskewitz, A. Grefhorst, et al., A novel approach to monitor glucose metabolism using stable isotopically labelled glucose in longitudinal studies in mice, Lab. Anim. 47 (2013) 79–88.
[9] A. Dikkers, J. Freak de Boer, W. Annema, et al., Scavenger receptor BI and ABCG5/G8 differentially impact biliary sterol secretion and reverse cholesterol transport in mice, Hepatology 58 (2013) 293–303.
[10] L.G. Dimova, J.F. de Boer, J. Plantinga, et al., Inhibiting cholesterol absorption during lactation programs future intestinal absorption of cholesterol in adult mice, Gastroenterology 153 (2017) 382–385 e3.
[11] N. Pomara, D. Bruno, A.S. Sarreal, et al., Lower CSF amyloid beta peptides and higher F2-isoprostanes in cognitively intact elderly individuals with major depressive disorder, Am. J. Psychiatry 169 (2012) 523–530.
[12] R.M. Lebovitz, H. Zhang, H. Vogel, et al., Neurodegeneration, myocardial injury, and perinatal death in mitochondrial superoxide dismutase-deficient mice, Proc. Natl. Acad. Sci. U. S. A. 93 (1996) 9782–9787.
[13] M.S. Winzell, B. Ahren, The high-fat diet-fed mouse: a model for studying mechanisms and treatment of impaired glucose tolerance and type 2 diabetes, Diabetes 53 (Suppl 3) (2004) S215–S219.
[14] S. Ishibashi, M.S. Brown, J.L. Goldstein, et al., Hypercholesterolemia in low density lipoprotein receptor knockout mice and its reversal by adenovirus-mediated gene delivery, J. Clin. Investig. 92 (1993) 883–893.
[15] L.A. Brondani, T.S. Assmann, G.C. Duarte, et al., The role of the uncoupling protein 1 (UCP1) on the development of obesity and type 2 diabetes mellitus, Arq. Bras. Endocrinol. Metabol. 56 (2012) 215–225.
[16] J. Wu, P. Bostrom, L.M. Sparks, et al., Beige adipocytes are a distinct type of thermogenic fat cell in mouse and human, Cell 150 (2012) 366–376.
[17] J.R. Jones, C. Barrick, K.A. Kim, et al., Deletion of PPARgamma in adipose tissues of mice protects against high fat diet-induced obesity and insulin resistance, Proc. Natl. Acad. Sci. U. S. A. 102 (2005) 6207–6212.
[18] K.S. Echtay, D. Roussel, J. St-Pierre, et al., Superoxide activates mitochondrial uncoupling proteins, Nature 415 (2002) 96–99.
[19] P. Puigserver, Z. Wu, C.W. Park, et al., A cold-inducible coactivator of nuclear receptors linked to adaptive thermogenesis, Cell 92 (1998) 829–839.
[20] A. Shore, A. Karamitri, P. Kemp, et al., Role of Ucp1 enhancer methylation and chromatin remodelling in the control of Ucp1 expression in murine adipose tissue, Diabetologia 53 (2010) 1164–1173.
[21] S.L. Dunwoodie, The role of hypoxia in development of the Mammalian embryo, Dev. Cell 17 (2009) 755–773.
[22] M. Ristow, K. Zarse, A. Oberbach, et al., Antioxidants prevent health-promoting effects of physical exercise in humans, Proc. Natl. Acad. Sci. U. S. A. 106 (2009) 8665–8670.
[23] M. Ristow, Unraveling the truth about antioxidants: mitohormesis explains ROS-induced health benefits, Nat. Med. 20 (2014) 709–711.
[24] S. Yu, E. Lee, B. Tsogbadrakh, et al., Prenatal hyperbaric normoxia treatment improves healthspan and regulates chitin metabolic genes in Drosophila melanogaster, Aging 8 (2016) 2538–2550.
[25] M. Tchirikov, E. Saling, G. Bapayeva, et al., Hyperbaric oxygenation and glucose/amino acids substitution in human severe placental insufficiency, Physiol. Rep. 6 (2018).
[26] J. Mao, X. Zhang, P.T. Sieli, et al., Contrasting effects of different maternal diets on sexually dimorphic gene expression in the murine placenta, Proc. Natl. Acad. Sci. U. S. A. 107 (2010) 5557–5562.
[27] H. Song, B.P. Telugu, L.P. Thompson, Sexual dimorphism of mitochondrial function in the hypoxic Guinea pig placenta, Biol. Reprod. 100 (2019) 208–216.